CHEMICAL ENGINEERING TRANSACTIONS
VOL. 56, 2017
A publication of AIDIC
The Italian Association of Chemical Engineering
Online at www.aidic.it/cet
Guest Editors: Jiří Jaromír Klemeš, Peng Yen Liew, Wai Shin Ho, Jeng Shiun Lim

ISBN 978-88-95608-47-1; **ISSN** 2283-9216
DOI: 10.3303/CET1756068

Photocatalytic Carbon Dioxide Reduction to Fuels Over Cu-Loaded g-C_3N_4 Nanocatalyst under Visible Light

Beenish Tahir, Muhammad Tahir, Nor Aishah Saidina Amin*

Chemical Reaction Engineering Group (CREG), Department of Chemical Engineering, Faculty of Chemical and Energy Engineering, Universiti Teknologi Malaysia, 81310 UTM Johor Bahru, Johor Malaysia.
*noraishah@cheme.utm.my

Photocatalytic carbon dioxide (CO_2) conversion to chemicals and fuels has gained significant consideration in industrial and scientific research. In this study, photocatalytic CO_2 reduction to fuels over Cu-loaded graphitic carbon nitride (g-C_3N_4) under visible light irradiation has been investigated. The photocatalysts, synthesized by pyrolysis and impregnation method, were characterized by X-ray diffraction (XRD) Fourier transform infrared (FTIR) and Scanning electron microscopy (SEM). Interestingly, CO_2 was efficiently converted to CH_4 and CH_3OH with smaller amounts of C_2H_4 and C_2H_6 hydrocarbons. The yield of CH_4 evolution as the main product over 3 wt. % Cu/g-C_3N_4 was 217.8 µmole/g.cat under visible light irradiation, significantly higher than the amount of CH_4 produced over the pure g-C_3N_4 catalyst (119 µmole/g.cat). The enhancement was attributed to charge transfer property and suppressed recombination rate by Cu-metal. The Cu-metal loaded into g-C_3N_4 enhanced CO_3 reduction efficiency for CH_4 production while the pure g-C_3N_4 was promising for both CH_4 and CH_3OH production. The single step conversion of CO_2 to CH_4 and CH_3OH with appreciable amount of hydrocarbons under solar energy registered good photo-activity and selectivity of Cu/g-C_3N_4 catalyst. A photocatalytic reaction mechanism was proposed to corroborate with the experimental results over the Cu-loaded g-C_3N_4 photocatalyst.

1. Introduction

Increasing levels of carbon dioxide (CO_2) emissions in the atmosphere from fossil fuel combustion are widely recognized as one of the primary cause of greenhouse effect. Among the carbon capture and sequestration, development of an artificial photosynthesis system using solar energy is a promising strategy for the photocatalytic conversion of CO_2 to solar fuels (Tahir et al. 2015b). Among the solar fuels, the production of CO (Tahir et al. 2016a), CH_4 (Zhu et al. 2016) and CH_3OH (Gusain et al. 2016) via a single step CO_2 conversion, has sparked a new sustainable development in the field (He et al. 2016).

Among the semiconductor materials, TiO_2 is the most widely studied photocatalyst due to its numerous advantages such as low cost and excellent chemical and thermal stability (Tahir et al. 2016b). However, TiO_2 is only active under UV-light irradiations and have poor photocatalytic activity due to the fast recombination of photo-generated charges (Tahir et al. 2015a). Considering the large portion of solar spectrum available, the demand for visible light responsive and low-cost photocatalysts has been regarded as an attractive area of research.

Recently, the use of graphitic carbon nitride (g-C_3N_4) as a photocatalyst has been promising alternatives due to advantages such as visible light responsive, low-cost synthesis and high chemical/thermal stability (Ma et al. 2016). In the recent years, there have been number of studies focused on photocatalytic CO_2 reduction by g-C_3N_4 based photocatalyst. However, the efficiency and selectivity of CO_2 conversion over pure g-C_3N_4 photocatalyst is still quite limited. The photocatalytic activity of g-C_3N_4 could be enhanced by loading with metals or combining with other semiconductor materials.

In this perspective, Pt-g-loaded C_3N_4/$kNbO_3$ photocatalyst has been recently investigated for enhanced CO_2 photoreduction under visible light irradiations (Shi et al. 2015). The amine-functionalized g-C_3N_4 has been reported to improve CO_2 adsorption capacity with enhanced activity for CO_2 photoreduction into CH_4 and CH_3OH (Huang et al. 2015). Similarly, selective photocatalytic CO_2 reduction to CH_3OH been reported using ZnO/g-C_3N_4 photocatalyst under visible light irradiations. The g-C_3N_4-N/TiO_2 photocatalyst has been investigated for

Please cite this article as: Tahir B., Tahir M., Amin N.A.S., 2017, Photocatalytic carbon dioxide reduction to fuels over cu-loaded g-c3n4 nanocatalyst under visible light, Chemical Engineering Transactions, 56, 403-408 DOI:10.3303/CET1756068

the selective CO_2 photoreduction to CO (Zhou et al. 2014). Pt-loaded g-C_3N_4 with improved day-light induced photocatalytic CO_2 reduction to CH_4 was explored. Significantly improved g-C_3N_4 photoactivity was found with Pt-loading, perhaps, due to hindered charges recombination rate (Ong et al. 2015). On the other hand, copper based semiconductors are gaining large interest and are considered as efficient for selective CO_2 photoreduction to CH_4 and CH_3OH (Liu et al. 2015). Therefore, it is anticipated that photocatalytic CO_2 reduction over Cu-promoted g-C_3N_4 catalyst would be appreciable to stimulate photocatalytic CO_2 reduction to selective fuels under visible light irradiations.

In this study, highly active and visible light responsive Cu-promoted g-C_3N_4 Nanosheets were successfully synthesized by thermal treatment of melamine. The photoactivity of different Cu-loaded g-C_3N_4 catalysts were examined for selective CO_2 photoreduction to fuels. In addition, the photocatalytic reaction mechanism for CO_2 reduction were analysed based on the experimental results.

2. Experimental

2.1 Catalyst preparation and characterization

The g-C_3N_4 was synthesized by the thermal treatment of Melamine (Sigma Aldrich AR ≥ 99%). In a typical process, 5 g of Melamine was put in a crucible with a cover then calcined in a Muffle Furnace and heated to 550 ^oC for 2 h. The sample was then washed with 0.1 mol/L nitric acid (Sigma Aldrich AR) and distilled water to remove any residual alkaline species (e.g. ammonia) adsorbed on the sample surface. After this, it was dried at 80 °C for 12 h in an oven. The Cu-loaded g-C_3N_4 samples were prepared by a wet-impregnation and sonication method. 0.5 g of g-C_3N_4 was dispersed in 20 mL water and specific amount of Cu $(NO_3)_2.3H_2O$ was added to it. The mixture was stirred for 4 h and then sonicated to get Cu-promoted g-C_3N_4 Nanosheets. The sample was oven dried at 80 °C for 12 h then calcined at 450 °C for 1 h.

The crystalline structure of the catalysts were ascertained by X-ray diffraction (XRD) recorded on a powder diffractometer (Bruker Advance D8, 40 kV, 40 mA) using a Cu Kα radiation source in the range of 2θ = 5-80 ° with a step size of 0.05 ° and counting time of 5 s. The Fourier transform infrared (FTIR) spectrum of the sample was recorded on a Thermo Nicolet Avatar 360 FTIR spectrometer. The surface morphology was examined using field emission scanning electron microscopy (FESEM JEOL model JSM-6700F, Japan).

2.2 Photoactivity testing

The reactor consists of stainless steel cylindrical vessel with a length of 5.5 cm and total volume of 150 cm^3. 10 mg powder photocatalyst was evenly placed inside the cylindrical stainless steel chamber, equipped with a quartz window for passing light irradiations. The source of light irradiation was a simulated sunlight having the same spectra with real sunlight. Compressed CO_2 (99.999 %) regulated by a mass flow controller (MFC) was bubbled through water saturator to carry moisture maintained at temperature of 30 ^oC. The reactor was purged and saturated for half an hour using a mixture of CO_2 and water prior to the start of the experiment. The temperature inside the reactor was controlled using temperature controller. The products were analyzed using an on-line gas chromatograph (GC-Agilent Technologies 6890 N, USA) equipped with thermal conductivity detector (TCD) and flame ionized detector (FID). Furthermore, FID detector was connected with a HP-PLOT Q capillary column and TCD detector was connected to UCW982, DC-200, Porapak Q and Mol Sieve 5A columns.

3. Results and discussion

3.1 Characterization analysis of catalysts

Figure 1 (a) presents the spectra of g-C_3N_4 and Cu/g-C_3N_4 samples and can be identified the presence of two peaks. The peak at 27.3 ° located at plane (002) presents interlayer stacked conjugated aromatic system, while the peak at ~ 13 ° with plane (100) reveals the intra-planar structural packing of the aromatic system. The signals corresponding to Cu in metal or oxides states were not detected in all the XRD patterns. This was possibly due to the lower amounts, which were below the detection limit of XRD or the Cu-species were highly dispersed over the g-C_3N_4 structure. Figure 1 (b) shows Infrared spectra of g-C_3N_4 and Cu-loaded g-C_3N_4 samples. All the spectra bands are attributed to the samples containing g-C_3N_4. An absorption band at 805 cm^{-1} is associated with the bending nodes of the parent structure of g-C_3N_4 in both the samples. The N-H stretch of the heterocyclic amines present in the g-C_3N_4 structure are identified by the bands at 1248-1571. The band located at 1,640 cm^{-1} can be attributed to the stretching vibration band of the C-N of amines in g-C_3N_4 (He et al., 2015).

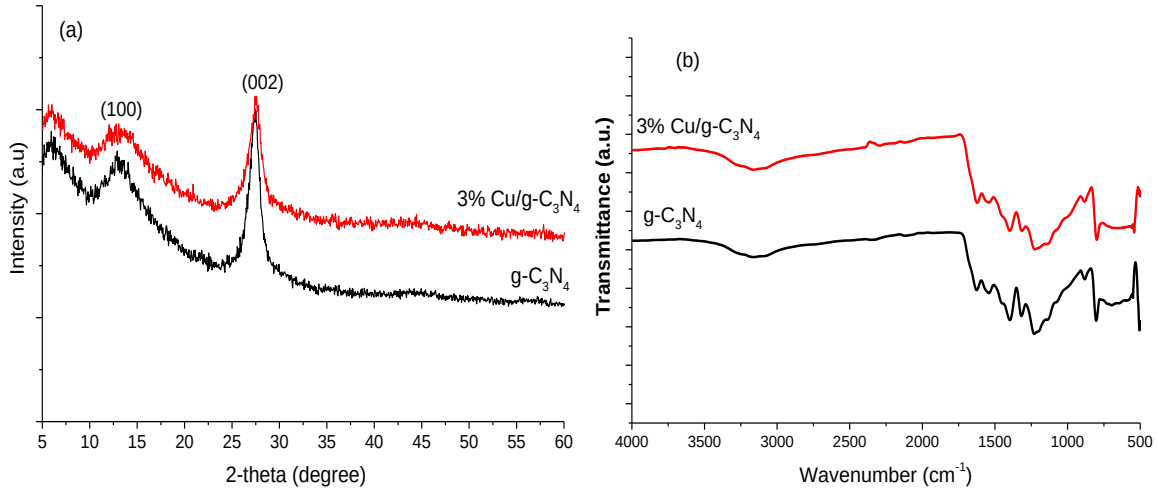

Figure 1: (a) XRD analysis of Cu/g-C_3N_4 samples; (b) FTIR spectra of the corresponding samples.

Figure 2 exhibits the morphology of pure and modified g-C_3N_4 samples. From Figure 2 (a), it can be seen that g-C_3N_4 has obvious lamellar and irregular folding structures like wrinkled sheets, in which layers are stacked together. Meanwhile, 3 % Cu/g-C_3N_4 in Figure 2 (b) depicts porous g-C_3N_4 layers of sheet-like structure. The slight disparity between the two samples is possibly due to effective stirring and sonication during metal impregnation of Cu/g-C_3N_4 sample.

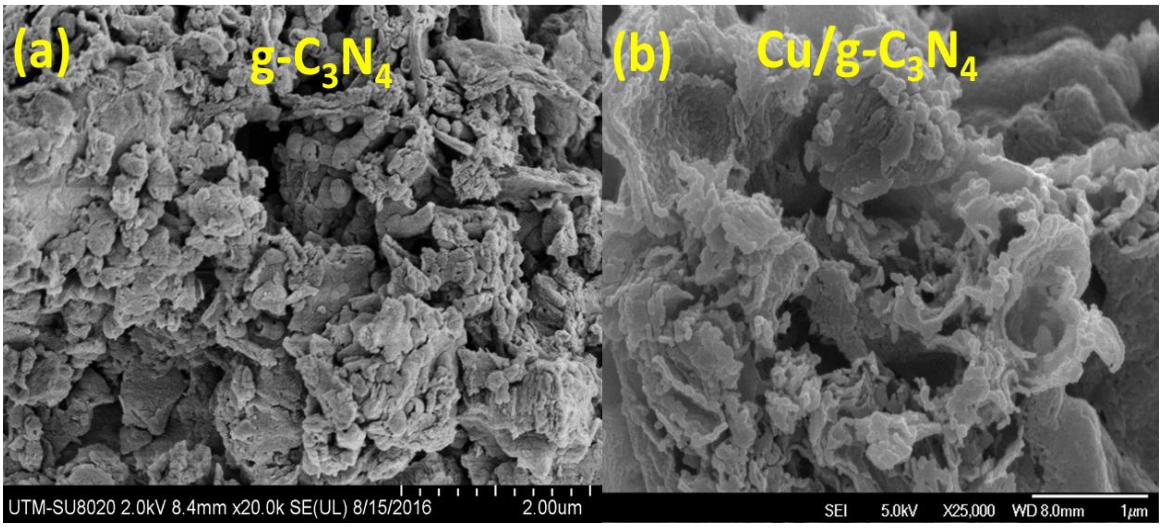

Figure 2: SEM images of Cu/g-C_3N_4 samples; (a) SEM image of g-C_3N_4, (b) SEM image of Cu/g-C_3N_4.

3.2 Photocatalytic CO_2 reduction with H_2O

Initially, blank experiments were conducted to confirm products formed were due to photoreduction of CO_2 only. Experiments were conducted in a gas phase system at 100 ^oC and irradiation time 2 h. In all types of catalysts, carbon containing compounds were not detected in the reaction system without reactants or light irradiations. Thus, any carbon containing compounds produced were derived from CO_2 photo-reduction with CH_4 and CH_3OH were found to be major CO_2 photo-reduction product in all the experiments.

The effects of Cu loading on the activity of g-C_3N_4 for CO_2 reduction to CH_4 and CH_3OH under visible light irradiations are presented in Figure 3.With pure g-C_3N_4, the yield of CH_4 is lower ,but gradually increases `with Cu loading until it attained an optimum yield at 3 wt. % Cu. With increasing Cu loading the yield decreases. This can be attributed to higher rates of charge recombination centres, resulting in reduced photoactivity (Liu et al. 2015).The effectiveness of Cu-loading was much appreciable for CH_4 production than the CH_3OH. On the other hand, yield of CH_3OH production gradually reduced with Cu-loading. The result indicates that the loading of the

pure catalyst (g-C_3N_4) with Cu metal become more efficient for CH_4 production, evidently due to reducing the band gap with hindered recombination rate of electron and hole pairs and ultimately increased in the product yield. However, pure g-C_3N_4 was more efficient for both CH_4 and CH_3OH production due to reason as discussed in reaction mechanism.

The effects of Cu onto g-C_3N_4 performance for CO_2 photo-reduction to hydrocarbons (C_2H_4 and C_2H_6) is presented in Figure 3 (b). Evidently, hydrocarbons were detected over all type of photocatalysts. However, Cu-loaded g-C_3H_4 have much appreciable effect of hydrocarbons production due to the more trapping and transport of electrons over Cu/g-C_3N_4 structure. Among the hydrocarbons, the yield of C_2H_6 was much higher in comparative to C_2H_4 and similar observation could be seen in all type of samples. This development has confirmed Cu-loaded g-C_3N_4 Nanosheets as a favourable visible light responsive photocatalyst for CH_4, CH_3OH and hydrocarbon production under solar energy.

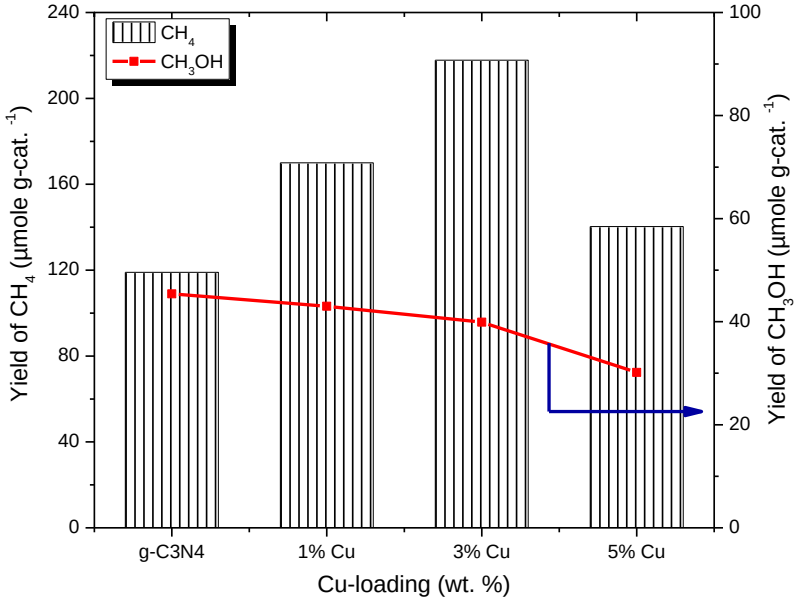

Figure 3: Effect of Cu loading onto the photoactivity of g-C_3N_4 Nanosheets for CO_2 reduction with H_2O to CH_4 and CH_3OH at 100 ^oC and irradiation time 2 h.

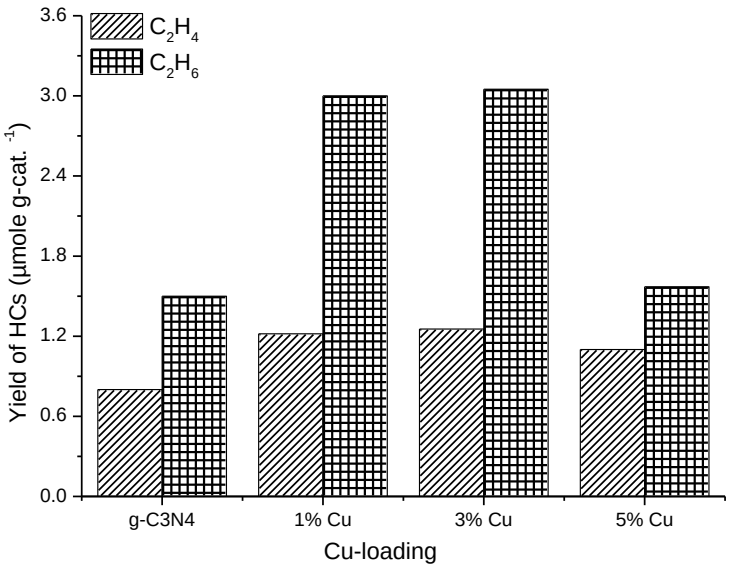

Figure 4: Photoreduction of CO_2 to hydrocarbons using H_2O reductant over Cu-loaded g-C_3N_4 samples under visible light irradiation and irradiation time 2 h.

3.3 Reaction mechanism

The multi-step reaction pathway of the process splits into three parts: the formation of the CO_2 radical, water splitting and formation of CH_4, CH_3OH and hydrocarbons. The feasible reaction pathway for this process is given by reactions in Eqs (1) – (8).

$$g\text{-}C_3N_4 \xrightarrow{\text{visible light}} e^- + h^+ \quad (1)$$

$$Cu^{2+} + 2e^- \longrightarrow Cu^{2+} / 2e^- \quad (2)$$

$$CO_2 + e^- \longrightarrow^{\circ} CO_2^- \quad (3)$$

$$H_2O + h^+ \longrightarrow \bullet OH + H^+ \quad (4)$$

$$CO_2 + 6H^+ + 6e^- \longrightarrow CH_3OH + H_2O \quad (5)$$

$$CO_2 + 8H^+ + 8e^- \longrightarrow CH_4 + 2H_2O \quad (6)$$

$$2CO_2 + 12H^+ + 12e^- \longrightarrow C_2H_4 + 4H_2O \quad (7)$$

$$2CO_2 + 14H^+ + 14e^- \longrightarrow C_2H_6 + 4H_2O \quad (8)$$

In the case of visible light irradiations, the photo-generated electrons and holes are produced over g-C_3N_4 photocatalyst. Eq (1) and (2) reveals photo-excited electron-hole pair production and their trapping by Cu-metal, resulting in prolonged lifetime of charges to precede oxidation and reduction process. The holes are used for oxidation of H_2O while electrons are consumed by CO_2 for its reduction as explained in Eq (3) and (4). Reactions in Eqs (5) to (8) divulged production of CH_4, CH_3OH and hydrocarbons through utilization of H+ ions and electrons in multi-step process.

The photocatalytic activity is related to the band structure and the mechanism for the production of these products over Cu/g-C_3N_4 photocatalyst is explained in Figure 5. Under the light irradiations, VB electrons of g-C_3N_4 can transfer to Cu-metal which cause electron-hole pair separation. This is due to the possibility of electron trapping by the copper ions as a result of the difference in reduction potential of Cu^{2+} which is more positive than the conduction band edge of g-C_3N_4 (-1.23 V vs. NHE). Since the reduction potential of CO_2/CH_3OH (-0.38 V) and CO_2/CH_4 (-0.24 V) are less than the conductance band of g-C_3N_4 (-1.23 V), thus production of these products are feasible. As discussed previously, g-C_3N_4 was favourable for CH_3OH production but copper has proven to be the preferred metal in the photoreduction of CO_2 to CH_4 as it demonstrates some level of selectivity for CH_4 production. Therefore, both reductant and metals are relatively important in photocatalytic CO_2 reduction applications for selective fuels.

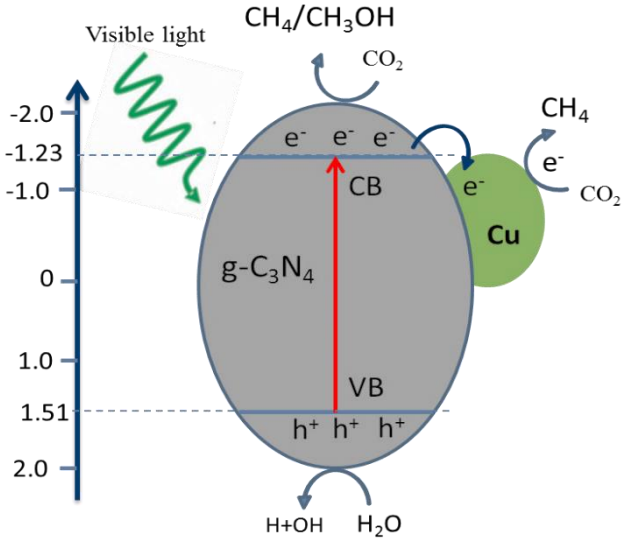

Figure 5: Schematic presentation of photocatalytic CO_2 reduction with H_2O to CH_4 and CH_3OH over Cu-loaded g-C_3N_4 photocatalyst under solar energy irradiations.

4. Conclusions

Cu-loaded g-C_3N_4 nanosheets were developed for gas phase photocatalytic CO_2 reduction by H_2O under visible light irradiation. The yield rate of CO_2 reduction increased significantly by introducing Cu into g-C_3N_4 catalyst. The yield rate of CH_4 as the key product over Cu/g-C_3N_4 was 217.8 μmole-g-cat.$^{-1}$, 1.83 fold higher when compared with pure g-C_3N_4 photocatalyst. Besides, significant amount of CH_3OH with appreciable amounts of C_2 hydrocarbons were also detected in the product mixture. The experimental results conferred that g-C_3N_4 is an efficient material functional under solar energy while Cu-promoted enhanced the photocatalytic CO_2 reduction to solar fuels.

Acknowledgement

We would like to express our sincere gratitude to the Ministry of Higher Education (MOHE), Malaysia for the financial support of this work made available through the Nanomite Long Term Research Grant Scheme (Nanomite LRGS) Project Vot 4L839.

References

Gusain R., Kumar P., Sharma O.P., Jain S.L., Khatri O.P., 2016, Reduced graphene oxide–CuO nanocomposites for photocatalytic conversion of CO2 into methanol under visible light irradiation, Applied Catalysis B: Environmental 181, 352-362.

He Y.M., Zhang L.H., Fan M.H., Wang X.X., Walbridge M.L., Nong Q.Y., Wu Y., Zhao L.H., 2015, Z-scheme SnO2-x/g-C3N4 composite as an efficient photocatalyst for dye degradation and photocatalytic CO2 reduction, Solar Energy Materials and Solar Cells 137, 175-184.

He Z.Q., Tang J.T., Shen J., Chen J.M., Song S., 2016, Enhancement of photocatalytic reduction of CO2 to CH4 over TiO2 nanosheets by modifying with sulfuric acid, Applied Surface Science 364, 416-427.

Huang Q., Yu J., Cao S., Cui C., Cheng B., 2015, Efficient photocatalytic reduction of CO2 by amine-functionalized g-C3N4, Applied Surface Science 358, 350-355.

Liu E.Z., Qi L.L., Bian J.J., Chen Y.H., Hu X.Y., Fan J., Liu H.C., Zhu C.J., Wang Q.P., 2015, A facile strategy to fabricate plasmonic Cu modified TiO2 nano-flower films for photocatalytic reduction of CO2 to methanol, Materials Research Bulletin 68, 203-209.

Ma D., Wu J., Gao M., Xin Y., Ma T., Sun Y., 2016, Fabrication of Z-scheme g-C3N4 /RGO/Bi2WO6 photocatalyst with enhanced visible-light photocatalytic activity, Chemical Engineering Journal 290, 136-146.

Ong W.J., Tan L.L., Chai S.P., Yong S.T., 2015, Heterojunction engineering of graphitic carbon nitride (g-C3N4) via Pt loading with improved daylight-induced photocatalytic reduction of carbon dioxide to methane, Dalton Transactions 44 (3), 1249-1257.

Shi H., Zhang C., Zhou C., Chen G., 2015, Conversion of CO2 into renewable fuel over Pt–g-C3N4/KNbO3 composite photocatalyst, RSC Advances 5 (113), 93615-93622.

Tahir B., Tahir M., Amin N.A.S., 2015a, Gold–indium modified TiO2 nanocatalysts for photocatalytic CO2 reduction with H2 as reductant in a monolith photoreactor, Applied Surface Science 338, 1-14.

Tahir M., Tahir B., 2016a, Dynamic photocatalytic reduction of CO2 to CO in a honeycomb monolith reactor loaded with Cu and N doped TiO2 nanocatalysts, Applied Surface Science 377, 244-252.

Tahir M., Tahir B., Amin N.A.S., 2015b, Gold-nanoparticle-modified TiO2 nanowires for plasmon-enhanced photocatalytic CO2 reduction with H2 under visible light irradiation, Applied Surface Science 356, 1289-1299.

Tahir M., Tahir B., Amin N.A.S., Muhammad A., 2016b, Photocatalytic CO2 methanation over NiO/In2O3 promoted TiO2 nanocatalysts using H2O and/or H2 reductants, Energy Conversion and Management 119, 368-378.

Zhou S., Liu Y., Li J., Wang Y., Jiang G., Zhao Z., Wang D., Duan A., Liu J., Wei Y., 2014, Facile in situ synthesis of graphitic carbon nitride (g-C3N4)-N-TiO2 heterojunction as an efficient photocatalyst for the selective photoreduction of CO2 to CO, Applied Catalysis B: Environmental 158-159, 20-29.

Zhu S.Y., Liang S.J., Bi J.H., Liu M.H., Zhou L.M., Wu L., Wang X.X., 2016, Photocatalytic reduction of CO2 with H2O to CH4 over ultrathin SnNb2O6 2D nanosheets under visible light irradiation, Green Chemistry 18 (5), 1355-1363.